

Disclaimer/Publisher's Note: The statements, opinions, and data contained in all publications are solely those of the individual author(s) and contributor(s) and not of MDPI and/or the editor(s). MDPI and/or the editor(s) disclaim responsibility for any injury to people or property resulting from any ideas, methods, instructions, or products referred to in the content.

Article

KDEL Receptor trafficking to the plasma membrane is regulated by ACBD3 and Rab4-GTP

Chuanding Tan^{1,2,†}, Yulei Du^{1,2,†}, Lianhui Zhu¹, Shuaiyang Jing^{1,2}, Jingkai Gao^{1,2}, Xihua Yue^{1,*}, Yi Qian^{1,*} and Intaeck Lee^{1,*}

¹ School of Life Science and Technology, ShanghaiTech University, Shanghai, China

² University of Chinese Academy of Sciences, Beijing, China

†These authors contributed equally to this work

* Correspondence: yuexh@shanghaitech.edu.cn; qianyi@shanghaitech.edu.cn; Lee-intaeck@ShanghaiTech.edu.cn

Abstract: KDEL receptor-1 maintains homeostasis in the early secretory pathway by capturing and retrieving ER-chaperones to the ER during heavy secretory activity. We have previously shown that a Golgi scaffolding protein (ACBD3) facilitates KDEL receptor localization at the Golgi via regulating cargo wave-induced cAMP/PKA-dependent signaling pathway. Unexpectedly, a fraction of the receptor is also known to reside in the plasma membrane as a stress response, although it is largely unknown exactly how KDEL receptor gets exported from the Golgi and travels to the PM. In this study, we sought to investigate the mechanism by which KDEL receptor gets exported from the Golgi *en route* to the PM and identified two crucial factors that greatly influence post-Golgi trafficking of KDEL receptor. We show here that ACBD3 depletion results in significantly increased trafficking of KDEL receptor to the PM via Rab4-positive tubular carriers emanating from the Golgi. Expression of constitutively activated Rab4 mutant (Q72L) increases surface expression of KDEL receptor up to 2~3-fold, whereas expression of GDP-locked Rab4 mutant (S27N) inhibits KDEL receptor localization to the PM. Importantly, KDELR trafficking from the Golgi to the PM is independent of PKA- and Src Kinase-mediated mechanism. Taken together, these results reveal that ACBD3 and Rab4-GTP are key players at the Golgi in regulating KDEL receptor trafficking to the cell surface.

Keywords: KDEL Receptor; ACBD3; Rab4; Rab11; Golgi; Plasma Membrane; Rab; trafficking; secretion

Introduction

Golgi apparatus plays essential roles in receiving newly synthesized proteins from the endoplasmic reticulum (ER) and delivering them to targeted destinations (1,2). During this highly coordinated process, some ER resident proteins are transported to the Golgi with nascent proteins and subsequently retrieved to the ER. A seven transmembrane Golgi protein, KDEL receptor (KDELR) recognizes a 'KDEL' signal motif, present in the C-termini of most soluble ER proteins and transports them from the Golgi to ER by coat protein complex I (COPI) vesicles (3-5).

At steady state, KDELR mostly localizes to the Golgi by a scaffold protein, acyl-CoA binding containing protein 3 (ACBD3) and maintains dynamic homeostasis in the early secretory pathway (6,7). Previous studies have reported that a small fraction of KDELR resides on the cell surface as well and circulates between the plasma membrane and the Golgi via a complex trafficking itinerary (8-11). Similar to canonical cell surface receptors, endocytosed KDELR is recycled to the plasma membrane via Rab GTPase-mediated early and recycling endosomal pathways. Rab proteins are critical components of the

machinery for membrane trafficking and involved in all steps from the initial cargo sorting to the final stage of fusion with destination membranes. Rab GTPases cycle between GTP-bound active and GDP-bound inactive states, which is catalyzed by guanine nucleotide exchange factors (GEFs) and GTPase activating proteins (GAPs) (12-14). Interestingly, studies have shown that the transport between the *trans*-Golgi network (TGN) and endosomes are bidirectional, and transport in each direction is regulated by Rab GTPases (15-18). It remains elusive whether KDELR exits the Golgi and transports to the plasma membrane via a Rab protein-mediated endosomal route.

The Golgi-to-ER retrograde transport of KDELR-containing ER proteins requires protein kinase A (PKA) phosphorylation of the C-terminus of KDELR, which in turn allows the recruitment of ArfGAP1/COPI proteins to the Golgi membranes and ensures the retrieval of KDELR ligands (19,20). Our previous study had shown that ACBD3, a putative PKA anchoring protein (AKAP), regulates KDELR-PKA interaction and ER traffic-induced retrograde transport of KDELR via ADP-ribosylation factor 1 (Arf1)-dependent tubulovesicular carriers (6). The Src tyrosine kinase has been shown to regulate KDELR retrograde transport to the ER(21). It has been reported the chaperone-KDELR stimulates a Golgi pool of Src-family kinases, which then in turn activate anterograde traffic through the Golgi(22). By now, there are several pathways involved in regulating KDELR retrograde trafficking including the KDELR ligand, Src, PKA, ARFGAP1 and ACBD3. However, it's unknown whether these mechanisms may be involved in regulating KDELR trafficking to the plasma membrane.

Here, we studied the role of the KDELR ligand, Src, PKA, ARFGAP1 and ACBD3 in regulating cell surface expression of KDELR. We show that only ACBD3 depletion greatly increase cell surface expression of KDELR. Live cell imaging results indicate that Golgi export of KDELR was carried out mostly by Rab4-labelled tubules. Overexpression of constitutively active Rab4 (Q72L) accelerated KDELR trafficking to the plasma membrane, whereas GDP-locked Rab4 mutant (S27N) inhibited KDELR expression at the PM. These results provide a novel insight for the mechanistic underpinning of Golgi-to-cell surface trafficking of KDELR.

Results

Surface expression of KDELR is greatly increased in ACBD3-depleted mammalian cell lines

To study the relationship between KDELR retrograde trafficking and its cell surface localization, we initially did a small scale screening of a number of proteins known to be involved in regulating KDELR retrograde trafficking to check their roles in regulating surface expression of KDELR at the plasma membrane. First, we tested surface expression of KDELR1-mCherry upon KDELR-ligand-induced relocation of KDELR to the ER. We co-transfected a secretory cargo fused to C-terminal KDEL sequence (hGH-GFP-KDEL) with KDELR1-mCherry overnight in HT1080 cells, followed by surface biotinylation protocol to examine surface expression of KDELR1 in these cells. The results showed that expression of hGH-GFP-KDEL caused decreased surface expression of KDELR1-mCherry compared to GFP or hGH-GFP control (**Figure 1A**). Both Src and PKA have been shown to regulate KDELR retrograde transport to the ER. Thus, we studied surface expression of KDELR1-mCherry while overexpressing a constitutive active mutant Src(E381G) or PKA- α . The results showed that both Src and PKA expression have no effect on surface expression of KDELR1-mCherry, compared to the control (**Figure 1B&C**). It has been reported that ARFGAP1 promotes sorting of KDELR1 and the formation of COPI vesicles(23-25). To determine the role of ARFGAP1 in regulating KDELR surface expression, we tested surface expression of KDELR1-mCherry after ARFGAP1 knockdown using RNA interference. The results showed that ARFGAP1 depletion had no effect on surface expression of KDELR1-mCherry, compared to the control (**Figure 1D**).

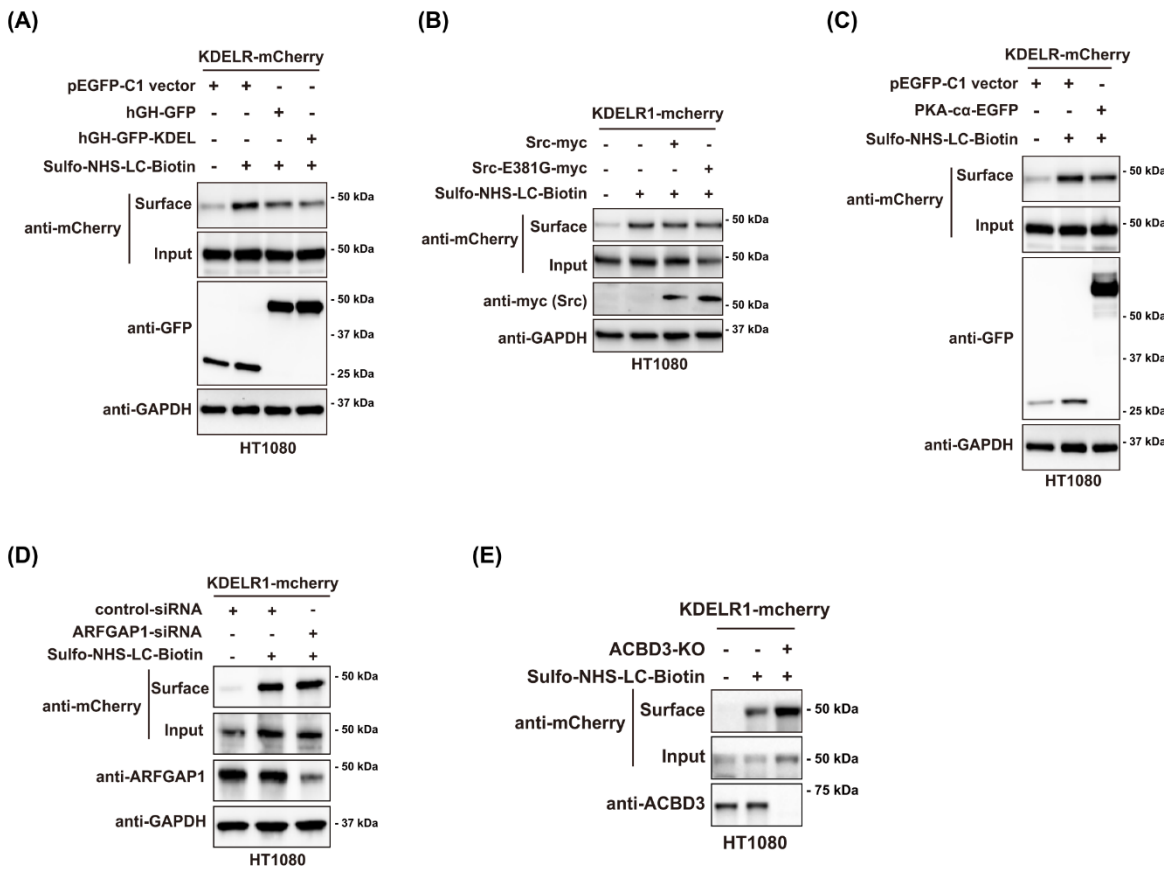


Figure 1. A small scale screening for potential regulators of KDELR trafficking to the plasma membrane. (A) Expression of hGH-GFP-KDEL causes decreased surface expression of KDELR1-mCherry compared to GFP or hGH-GFP control. HT1080 cells co-transfected with KDELR1-mCherry and hGH-GFP-KDEL, hGH-GFP or GFP control and cell surface expression of KDELR1-mCherry were detected by cell surface biotinylation. (B) HT1080 were co-transfected with KDELR1-mCherry and Src-WT or a constitutive active mutant E381G, followed by cell surface biotinylation. Biotinylated proteins were isolated by streptavidin-agarose and subjected to western blot analysis using the indicated antibodies. (C) HT1080 cells co-transfected with KDELR1-mCherry and PKA-α-EGFP or EGFP control and cell surface expression of KDELR1-mCherry was detected by cell surface biotinylation. (D) HT1080 cells were transfected with ARFGAP1 siRNA for 48h, then transfected with KDELR1-mCherry for 18 hours, followed by cell surface biotinylation. Biotinylated proteins were isolated by streptavidin-agarose and subjected to western blot analysis using the indicated antibodies. (E) WT or ACBD3-KO HT1080 cells were transfected with KDELR1-mCherry for 18 hours, followed by cell surface biotinylation. Biotinylated proteins were isolated by streptavidin-agarose and subjected to western blot analysis using the indicated antibodies.

In our earlier study, we reported that ACBD3 plays a key role in suppressing PKA activity on KDELR, thereby facilitating Golgi localization of KDELR under steady state condition (6). To study whether ACBD3 may be involved in the receptor export from the Golgi to the PM, we tested surface expression of KDELR1-mCherry in ACBD3 knockout HT1080 cells using surface biotinylation protocol (11). The results showed that ACBD3 knockout greatly increases surface expression of KDELR1-mCherry (**Figure 1E**). To confirm this result, we tested surface expression of KDELR1-mCherry after ACBD3 knockdown in several other cell lines. To this end, five human cell lines including HeLa-S3, human lung cancer cell A549, human prostate cancer cell DU145, human hepatoma HepG2 and human osteosarcoma U-2 OS were treated with shRNA lentivirus to stably knock down ACBD3. We then transiently transfected the cells with KDELR1-mCherry overnight, followed by surface biotinylation protocol to examine surface expression of KDELR1 in these cells. The results showed that all five cell lines displayed 1.5~3-fold increase in surface expression of KDELR1-mCherry upon ACBD3 depletion (**Figure 2A-E**), while expression of shRNA-resistant myc-ACBD3 completely restored KDELR1 surface expression to that of the control cells (**Figure 2F**). To confirm this finding by confocal

microscopy, we transiently co-transfected ACBD3 KD HeLa-S3 cells as well as ACBD3 KO cells (6) with lumenally 3xFlag-tagged KDELR-mCherry (Figure 2G) and YFP-GL-GPI (as a PM marker) overnight, followed by indirect immunostaining using anti-Flag antibody, in order to measure surface expression of KDELR1 in these cells. Upon examination by confocal microscope, both ACBD3 KD and KO resulted in significant increased surface expression of KDELR1 (Figure 2H), further confirming the earlier results by surface biotinylation experiments.

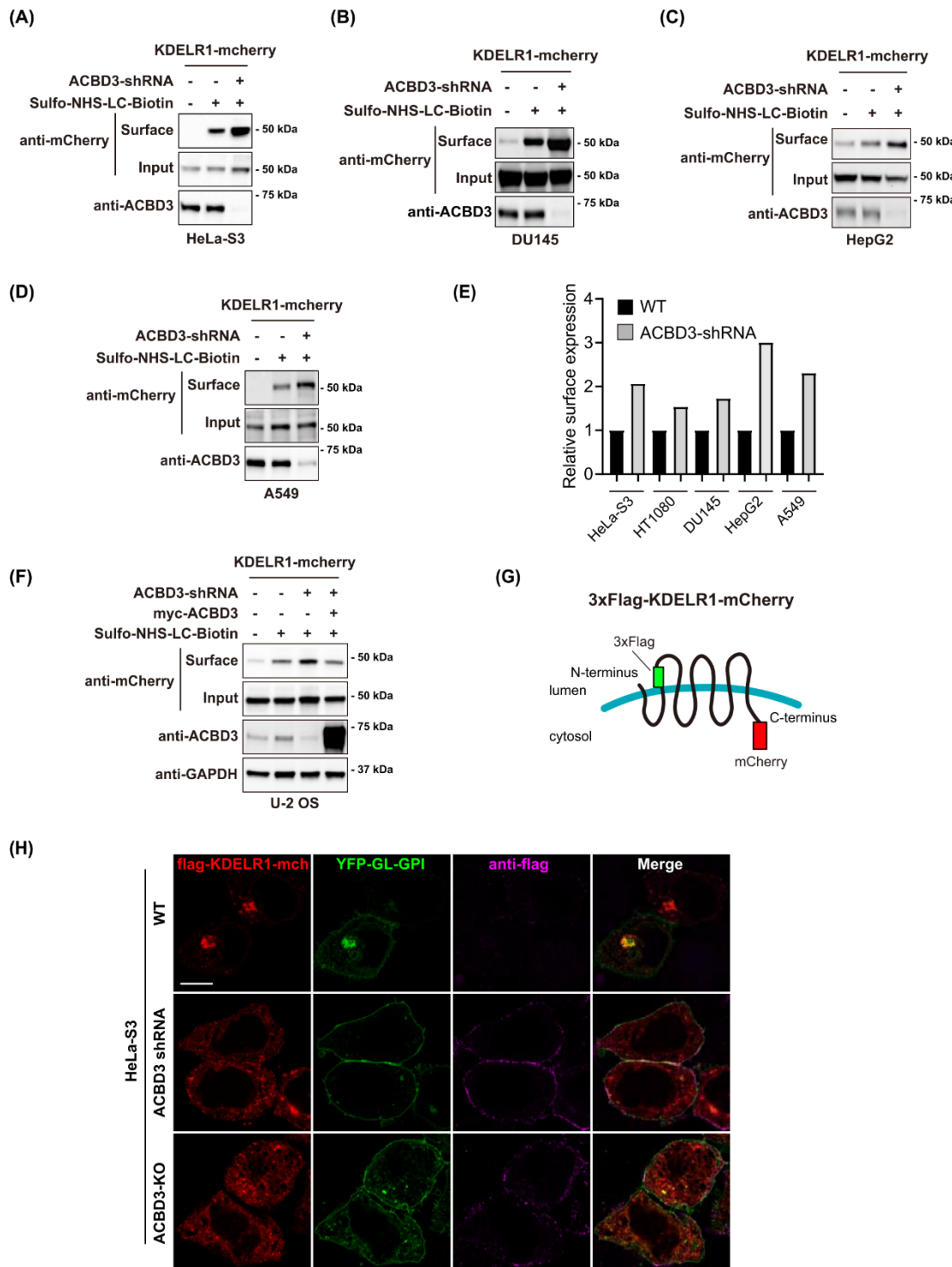


Figure 2. ACBD3 depletion results in significantly increased expression of KDELR on the cell surface. (A-D) Cell surface expression of KDELR1-mCherry is significantly increased in a number

of ACBD3 depleted cell lines, compared to the control cells. Cell surface expression of KDELR1-mCherry was probed by cell surface biotinylation protocol using sulfo-NHS-LC-biotin. We used shRNA/lentiviral transduction method to establish four mammalian cell lines, for which ACBD3 was stably knocked down, as described in the Methods. Briefly, WT or ACBD3 depleted cells were transfected with KDELR1-mCherry for 18 hours, followed by cell surface biotinylation. Biotinylated proteins were isolated by streptavidin-agarose and subjected to western blot analysis using the indicated antibodies. (E) Bar graphs showing normalized cell surface expression of KDELR-mCherry in various cell lines using densitometric analysis. (F) Cell surface expression of KDELR1-mCherry is significantly increased in ACBD3 depleted U-2 OS cells, compared to the control cells, which could be restored by exogenous expression of RNAi-resistant myc-ACBD3. (G) Schematic representation of 3xFLAG-KDELR1-mCherry. 3xFLAG tag was inserted into the first luminal (extracellular) loop of KDELR1. (H) Increased cell surface staining of 3xFLAG-KDELR1 observed by confocal microscopy in ACBD3-knockdown/knockout HeLa S3 cells. Control or ACBD3-knockdown/knockout HeLa S3 cells were co-transfected with 3xFLAG-KDELR1-mCherry and YFP-GL-GPI, which served as a cell surface marker, for 18 hours. The living cells were stained by anti-FLAG tag antibody at 4 °C and fixed with 4% paraformaldehyde, followed by staining with the secondary antibodies. Scale bars = 10 μ m.

Rab4-positive tubular emanations overlap well with KDELR-containing tubular emanations from the Golgi

As it is possible that ACBD3 depletion somehow stimulates Rab14- and Rab11-dependent KDELR recycling pathways for surface-expressed pool of the receptor (11), leading to increased expression of KDELR at the PM, we performed live cell imaging to investigate whether export of Golgi-localized KDELR are being influenced by ACBD3 depletion. Thus, we co-transfected either the control HT1080 cells or stable ACBD3 KD HT1080 cells (using shRNA lentivirus) with KDELR1 fused to photoactivatable GFP (PA-GFP) and mCherry-Rab4 (**Figure 3A-B**), mCherry-Rab14 (**Figure 3C-D**), mCherry-Rab11 (**supplementary Figure 1**), respectively. We then used a 405 nm laser to activate the Golgi-localized pool of KDELR1-PA-GFP and track the formation of Golgi-derived, KDELR1-positive tubulovesicular carriers using live imaging protocol, as described in the methods.

Upon examination using live cell confocal imaging, we found greatly increased frequency in KDELR1-positive tubulovesicular carrier formation in ACBD3 KD cells, compared to the control cells (**Figure 3E**) (6). Unexpectedly, Golgi-derived KDELR1-positive tubular carriers showed relatively poor overlap with either mCherry-Rab14 or Rab11 (**Figure 3E**), indicating that increased targeting of KDELR1 to the PM in ACBD3-depleted cells may not result from elevated rate of Rab14- and Rab11-mediated KDELR recycling to the PM. Instead, Golgi-derived KDELR1-positive tubular emanations overlapped very well with mCherry-Rab4 (**Figure 3A-B, E**), suggesting that KDELR1 export from the Golgi may be facilitated by Rab4.

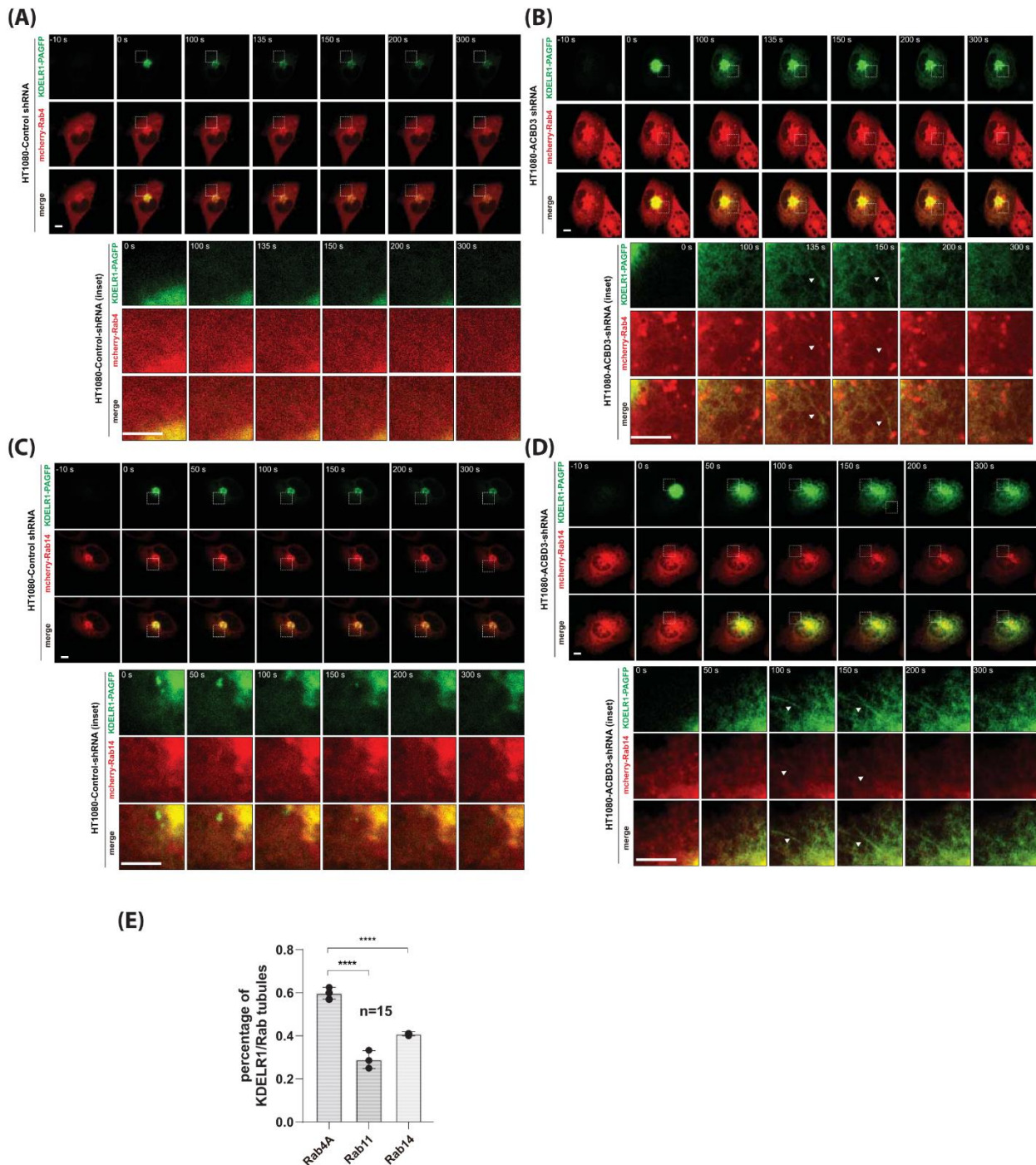


Figure 3. ACBD3 depletion results in increased trafficking of KDEL receptor to the PM via Rab4-positive tubular carriers at the Golgi. (A-D) To examine the post-Golgi trafficking itineraries of KDEL receptor to the PM, WT or ACBD3-depleted HT1080 cells were co-transfected with photoactivatable KDELR1-PA-GFP and mCherry-Rab4A/14 plasmids for 18 hours. The KDELR1-PA-GFP in the Golgi were then activated by selecting an ROI of mCherry-Rab4A/14 perinuclear region for intense 405 nm laser irradiation and the transport out of the Golgi are monitored by live cell imaging acquired every 5 seconds for 5 min. Imaging sequences prior to photoactivation (-10 seconds), immediately after photoactivation (0 second) and the indicated time points following photoactivation are presented here. Magnified regions of interest (indicated by white boxes) from WT and ACBD3-KO cells at the indicated time points shows Golgi-derived tubules which are highlighted by white arrowheads. Scale bars = 5 μ m. (E) Bar graphs showing the percentage of KDELR1/Rab tubules present in ACBD3-depleted HT1080 cells. N = 15 cells. Statistical analysis was performed using one-way ANOVA with a Tukey's post-hoc test (mean \pm SD; ****, p<0.0001).

Rab4 co-localizes with Golgi markers and mediates KDELR-positive, Golgi-derived tubular carrier formation

Rab4 had been shown to primarily mediate fast recycling pathways at the early endosomes for various surface expressed receptors (26,27), but not to mediate receptor trafficking at the Golgi. Interestingly, Rab4 also orchestrates Arl1-dependent BIG1/BIG2 recruitment and formation of clathrin adaptor (AP-1, AP-3 and GGA-3)-enriched endosomal sorting domain (28), which had been known to predominantly occur at the TGN (29-34). In order to find out whether Rab4 is associated with the Golgi membrane, we examined co-localization of mCherry-Rab4 (both human and mouse) with various Golgi markers using confocal. The results showed that a perinuclear pool of mCherry-Rab4 co-localized well with both GM130 and Golgin97 (Golgi markers) in HT1080 cells (to a lesser extent in HeLa-S3 cells), suggesting that a fraction of Rab4 may localize to the Golgi membranes and be involved in Golgi-derived tubular carrier formation (**Figure 4A-C**).

As Rab4 seems playing an important role in KDELR export from the Golgi, we then posited that exogenous over-expression of constitutively active Rab4 may stimulate surface targeting of KDELR1. To focus on Golgi-associated pool of KDELR and Rab4, HT1080 cells were transiently co-transfected overnight with KDELR1-PA-GFP and mCherry-Rab4-Q72L, followed by photoactivation using a 405 nm laser and live imaging protocol, as described in the methods. The results showed that a significant fraction of Golgi-derived KDELR tubules overlapped with mCherry-Rab4A-Q72L in WT HT1080 cells, suggesting that Rab4-Q72L expression stimulates KDELR export from the Golgi, rather than at the early endosome (**Figure 4D**).

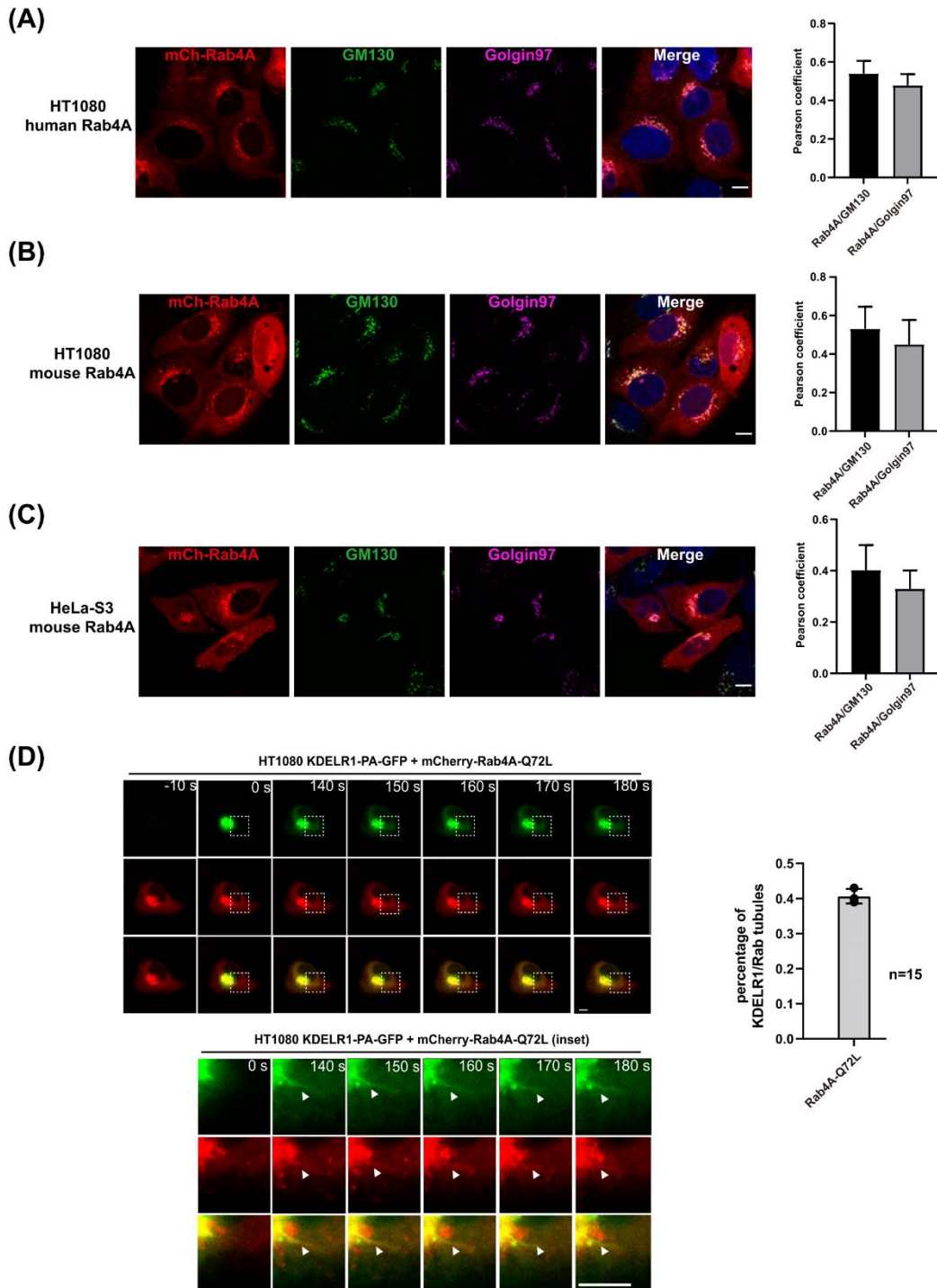


Figure 4. Overexpression of a constitutive active mutant Rab4-Q72L promotes KDELR1 trafficking to the PM via Rab4-positive tubular carriers at the Golgi. (A-C) To examine Golgi localization of Rab4A, HT1080 or HeLa-S3 cells were transfected with human or mouse mCherry-Rab4A plasmids for 18 hours, followed by staining with anti-GM130 (*cis*-Golgi) and anti-Golgin97 (*trans*-Golgi). Scale bars = 10 μ m. Co-localization (Pearson's R) was determined. N = 20. (D) To examine the role of Rab4 in promoting KDELR1 trafficking to the PM from Golgi, WT HT1080 cells were co-transfected with photoactivatable KDELR1-PA-GFP and mCherry-Rab4A-Q72L plasmids for 18 hours. The KDELR1-PA-GFP in the Golgi were then activated by selecting an ROI of mCherry-Rab4A Golgi region for intense 405 nm laser irradiation and the transport out of the Golgi were monitored by live cell imaging acquired every 5 seconds for 5 min. Imaging sequences prior to photoactivation (-10 seconds), immediately after photoactivation (0 second) and the indicated time points following photoactivation are presented here. Magnified regions of interest (indicated by white boxes) at the indicated time points shows Golgi-derived tubules which are highlighted by white arrowheads. Scale

bars = 5 μ m. Bar graphs showing the percentage of KDELR1/Rab tubules present in HT1080 cells. N = 15 cells. Statistical analysis was performed using two-tailed, paired t.test (mean \pm SD, ***, p<0.001).

Constitutively active Rab4-Q72L greatly increase surface expression of KDELR, whereas expression of GDP-locked Rab4 mutant inhibits KDELR expression on the cell surface

To further confirm these results, we then transfected HT1080 cells with either mCherry-Rab4-Q72L or S27N (GDP-locked mutant) overnight and checked whether KDELR1 trafficking to the PM may be influenced by the Rab4 mutant expression using surface biotinylation protocol. The results indeed indicated that Rab4-Q72L mutant expression greatly increase KDELR1 expression at the PM by several fold, whereas S27N mutant failed to do so (**Figure 5A**), as shown by surface biotinylation experiments. As controls, we also performed similar experiments with Rab11-Q70L/S25N and Rab14-Q70L/S25N mutant pairs, but did not see any meaningful changes in the surface expression of KDELR1 in these cells (**Figure 5B-C**), which helped us exclude the possibility of any potential misinterpretation from Rab-cascades (35).

In an effort to obtain more quantitative measure of KDELR expression on the PM, HT1080 cells were co-transfected with lumenally FLAG-tagged KDELR1-mCherry and EGFP-Rab4-Q72L or Rab4-S27N mutants, followed by indirect staining using anti-Flag antibody. Upon examination by confocal microscope, we found that anti-FLAG tag staining for surface-expressed KDELR were readily observed in HeLa-S3 cells transfected with Rab4-Q72L, but not detected for the cells transfected with Rab4-S27N or Rab7-Q67L (a control; N=40) (**Figure 5D-E**), again confirming that Rab4 is a major regulator of KDELR1 trafficking from the Golgi to the PM.

We then asked whether GDP-locked Rab4 mutant can inhibit KDELR trafficking to the cell surface in ACBD3 KD cells. To this end, HT1080 cells were transfected with EGFP-Rab4A-S27N mutant or pEGFP vector control, followed by surface biotinylation protocol to measure its influence on KDELR expression on the PM. Strikingly, expression of Rab4 S27N mutant alone significantly reduced basal surface expression of KDELR (**Figure 5F**; lane 1-3). In cells depleted of ACBD3, surface expression of KDELR was also reduced to a similar extent by Rab4-S27N expression (**Figure 5F**; lane 5-6). Taken together, these results suggested that Rab4-mediated regulation of KDELR trafficking most likely work at the downstream of ACBD3.

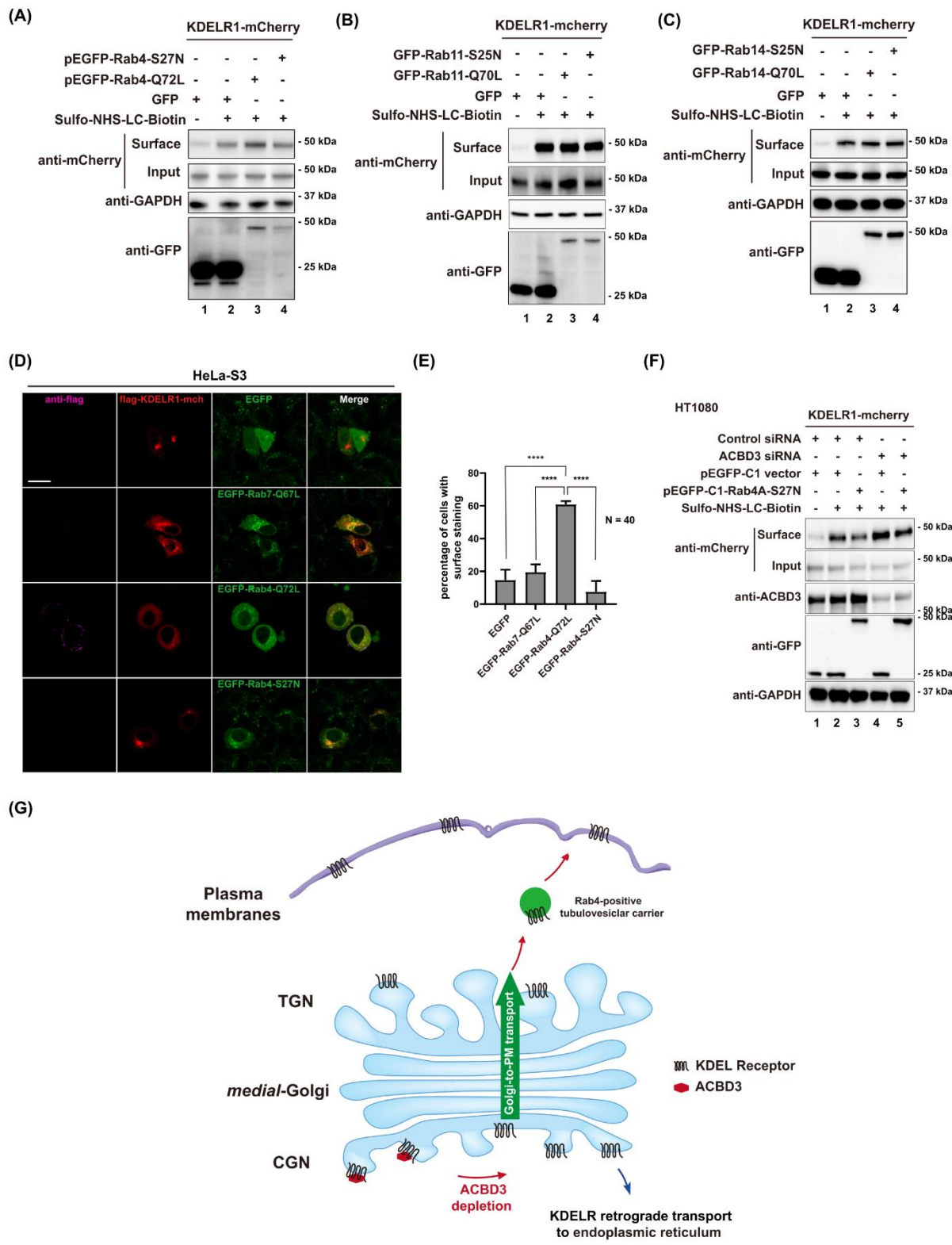


Figure 5. Rab4 plays a crucial role in cell surface expression of KDELR1. (A-C) Cell surface expression of KDELR1-mCherry is significantly increased in HT1080 cells when overexpressing constitutive active mutant Rab4A-Q72L, but not Rab11-Q70L or Rab14-Q70L, compared to the control cells. HT1080 cells were transfected with KDELR1-mCherry and indicated Rab plasmids for 18 hours, followed by cell surface biotinylation. Biotinylated proteins were isolated by streptavidin-agarose and subjected to western blot analysis using the indicated antibodies. (D) Increased cell

surface staining of 3xFLAG-KDELR1 observed by confocal microscopy in HeLa S3 cells expressing constitutive active mutant Rab4A-Q72L, compared to the cells expressing pEGFP-C1 vector, EGFP-Rab7-Q67L or EGFP-Rab4-S27N. HeLa S3 cells were co-transfected with 3xFLAG-KDELR1-mCherry and pEGFP-C1 vector or indicated Rab plasmids for 18 hours. The living cells were stained by anti-FLAG tag antibody at 4 °C and fixed with 4% paraformaldehyde, followed by staining with the secondary antibodies. Scale bars = 5 μ m. (E) Bar graphs showing the percentage of cells with surface staining of KDELR1 in 3xFLAG-KDELR1-mCherry transfected HeLa-S3 cells. N = 40 cells. Statistical analysis was performed using one-way ANOVA with a Tukey's post-hoc test (mean \pm SD; ****, p<0.0001). (F) Cell surface expression of KDEL-R1-mCherry is decreased in both HT1080 WT or ACBD3 knockdown cells when overexpressing a dominant negative mutant Rab4A-S27N. HT1080 cells were transfected with control siRNA or ACBD3 siRNA for 48h. Then cells were transfected with KDELR1-mCherry and EGFP-Rab4A-S27N or pEGFP-C1 vector plasmids for 18 hours, followed by cell surface biotinylation. Biotinylated proteins were isolated by streptavidin-agarose and subjected to western blot analysis using the indicated antibodies. (G) Schematic diagram depicting the proposed role of ACBD3 in controlling KDELR trafficking to the PM.

Discussion

We had previously shown that surface expressed KDELR undergoes clathrin-mediated endocytosis and highly complex recycling pathways through the endo-lysosomal system, including Rab11- and Rab14-positive recycling endosomes (11). In that study, we also found that the internalized pool of surface expressed KDELR doesn't utilize Rab4-dependent fast recycling pathway through the early endosomes. Therefore, it is interesting to note that Golgi exit of KDELR preferentially uses Rab4-dependent tubular carriers over Rab11- and Rab14-dependent mechanism. Co-localization analysis using Golgi markers (GM130 and Golgin97; **Figure 4A-C**) and live cell imaging results using KDELR-PA-GFP and mCherry-Rab4A-Q72L (**Figure 4D**) indicate that (i) there is a small subset of Rab4 pool associated with the Golgi membranes; (ii) constitutively active Rab4-Q72L expression induces frequent KDELR-positive tubular emanations from the Golgi, instead of the early endosomes, as had been widely accepted previously (26,28,36).

While we cannot exclude a possibility that Rab4-Q72L expression could accelerate the fast recycling route of internalized surface expressed KDELR, leading to increased KDELR expression on the PM, our live imaging results suggest that Rab4-mediated export of Golgi-localized KDELR to the PM is also likely to contribute directly to increased KDELR expression on the cell surface.

In addition, as both Rab11-Q70L and Rab14-Q70L expression had negligible influence on surface expression of KDELR (**Figure 5B-C**), there is little reason to believe that Rab4-Q72L-induced tubular carrier containing KDELR (**Figure 4D**) may be derived from the perinuclear recycling endosomes, instead of the Golgi. Thus, we conclude that Rab4 may mediate Golgi exit of certain recycling receptors at the TGN (**Figure 5G**), which has been overlooked so far (26,27,37-39).

How does ACBD3 regulate surface expression of KDELR? Since ACBD3 control KDELR localization to the Golgi under steady state condition by modulating its interaction with PKA (6), we initially hypothesized that PKA (or activation of related Src kinase-dependent signaling (40)) may dictate KDELR exit from the TGN. Unexpectedly, however, we found that either over-expressing PKA C α or expression of Src-E381G-myc had negligible effect on surface expression of KDELR (**Figure 1B&C**). Overall, it is not yet clear if other unknown KDEL cargo-induced signaling pathway may exist and regulate Golgi exit of KDELR.

It is possible that physical association between KDELR and ACBD3 may exert an inhibitory influence, effectively minimizing Golgi leakage of KDELR under steady state condition. Since ACBD3 is known to localize throughout the Golgi, including the TGN (41-43), this is a possibility, although the mechanism of KDELR release from ACBD3 is currently poorly understood.

Alternatively, since ACBD3 depletion greatly increases Arf1-positive tubular carrier formation (6), we suspect that increased Arf1 activity in ACBD3-depleted cells may partly

explain increased KDELR export from the Golgi, although this requires an in-depth further study.

Recently, KDELR was shown to promote FAK recruitment and activation to the area of ECM degradation in invadopodia and also stimulate directed vesicular trafficking and protrusive membrane dynamics at the PM (44,45). Moreover, secreted ER chaperones, such as ERp57 and GRP78, were reported to stimulate cancer cell migration and invasion, in which the latter was shown to promote ECM degradation and FAK activation as well (46-48). Thus, it would be intriguing to investigate whether surface expressed KDELR may interact with secreted ER-chaperones and facilitates invasive behavior of various cancers. In this context, it is worth noting that ACBD3, Arf1, PI4K β and Rab4 have all been implicated in breast cancer progression and prognosis and found to be coordinately regulated in the same region of Chromosome 1q (49-54).

In conclusion, our new results shed light on a previously unknown mechanism for post-Golgi trafficking of KDELR to the cell surface, which may play an important role in promoting secreted ER-chaperone-induced cell migration and invasion of several cancer cells.

Materials and Methods

Cell culture and transfection

HeLa S3 obtained from ATCC was grown in Delbecco's modified Eagle medium (DMEM, Meilunbio) supplemented with 10% fetal bovine serum (FBS, EXCELL). HepG2, DU145 and HT-1080 (Stem Cell Bank, Chinese Academy of Sciences) were grown in Minimum Essential Medium (MEM, Meilunbio) supplemented with 10% FBS. A549 (Stem Cell Bank, Chinese Academy of Sciences) was grown in F-12K (Meilunbio) supplemented with 10% FBS. U-2 OS (Meilunbio) was grown in McCoy's 5A (Meilunbio) supplemented with 10% FBS. HeLa S3 cells were authenticated by STR profiling. The authentication of other cell lines are provided by the provider. All cell lines were routinely tested for the mycoplasma contamination and were negative. Transfection of DNA constructs and siRNAs was performed using Lipofectamine 2000 and RNAi-MAX (ThermoFisher), respectively, according to the manufacturer's instructions. For DNA expression, cells were transfected 18h for immunofluorescence (IF) experiments. For siRNA knockdown, cells were transfected 72 h before experiments.

Antibodies, reagents, siRNAs, shRNA and CRISPR knockout

Following antibodies were used in this study: anti-ACBD3 (HPA015594, Sigma-Aldrich), anti-mCherry (ab167453, Abcam), anti-GFP (ab6556, Abcam), anti-Flag (F1804, Sigma-Aldrich), anti-Myc-tag (2278S, CST), anti-GFP (ab6556, Abcam), anti-ARFGAP1 (ab204405, Abcam), anti-PKA- α (#4782, Cell Signaling Technology), anti-EGFR (4267s, Cell Signaling Technology), anti-GAPDH-HRP (HRP-60004, Proteintech).

The siRNAs were custom designed by Shanghai GenePharma, China. The sequence of the non-targeting control siRNA was UUCUCCGAACGUGUCACGU. The sequences are as follows: ACBD3 siRNA-1: GCAUUAGAGUCACAGUUUA, ACBD3 siRNA-2: GCUGAACGUUACAUGAGCUA; ARFGAP1 siRNA-1: AAGGUGGUGCGCU-CUGGCCGAAG, ARFGAP1 siRNA-2: GCAACAUAGACCAGAGCUU; We combined siRNA-1 and siRNA-2 to get high knockdown efficiency for the experiments. The stable knockdown of ACBD3 was achieved by infecting target cells using lentivirus expression of ACBD3-shRNA (GCTGAAGTTACATGAGCTACA). The lentivirus was packaged and commercially provided by Shanghai GenePharma, China. Cells were infected with the lentivirus expressing ACBD3-shRNA using Polybrene (Sigma) overnight. Two days after infection, the cells were cultured in puromycin (0.3–1 μ g/ml, ThermoFisher) for 2 weeks.

CRISPR knockout of ACBD3 in HT1080 and HeLa-S3 cells were performed as described previously(6).

Cell surface biotinylation

Cells grown in 6-well plates to 80% confluency were transfected using 0.8 µg plasmid DNA and 3 µl Lipofectamine 2000 for 18 h. During the biotinylation procedure, all reagents and cell cultures were kept on ice. Cells were washed twice in ice-cold PBS and subsequently incubated in 1 ml/well of a 1 mM Sulfo-NHS-LC-Biotin (APEXBIO) in PBS solution for 30 min on ice. The cells were then washed in quenching buffer (100 mM glycine in PBS), and incubated in 1 ml/well of quenching buffer for 15 min on ice. The cells were washed twice with PBS and then lysed in 300 µl RIPA lysis buffer (50mM Tris, pH 7.4, 150mM NaCl, 0.1% SDS, 1% (v/v) Triton X-100, 0.5% (w/v) deoxycholate, and protease inhibitor cocktail (Roche)). Lysates were incubated for 20 min on ice and sonicated for 20 seconds. Finally, the lysate was centrifuged at 4°C for 10 min at 15000xg. Supernatants were incubated with 40 µl of Streptavidin Agarose beads (S1638, Sigma Aldrich) with constant rocking for 1 h at 4 °C. The samples were washed three times with PBS, then eluted with 2x SDS-sample buffer for 10 min at 95 °C and used for Western blot.

Immunoblotting

For immunoblotting, proteins were separated by SDS-PAGE (Genscript) and transferred onto nitrocellulose membranes (Amersham). Membranes were probed with specific primary antibodies and then with peroxidase-conjugated secondary antibodies (Jackson ImmunoResearch). The bands were visualized with chemiluminescence (Clarity Western ECL Substrate, Bio-Rad) and imaged by a ChemiDoc Touch imaging system (Bio-Rad). Representative blots are shown from several experiments.

Immunofluorescence staining and confocal microscopy

Cells grown on glass coverslips in 24-well plates were fixed for 10 min with 4% paraformaldehyde (PFA), permeabilized in permeabilization Buffer (0.3% Igepal CA-630, 0.05% Triton-X 100, 0.1% IgG-free BSA in PBS) for 3 min, then blocked in blocking buffer (0.05% Igepal CA-630, 0.05% Triton-X 100, 5% normal goat serum in PBS) for 60 min. Primary and secondary antibodies were applied in blocking buffer for 1 hour. The nucleus was stained with Hoechst-33342 (sc-200908, Santa cruz Biotechnology). Cells were washed three times with wash buffer (0.05% Igepal CA-630, 0.05% Triton-X 100, 0.2% IgG-free BSA in PBS) and twice with PBS. Coverslips were mounted using ProLong Gold Antifade Reagent (ThermoFisher).

For cell surface staining of 3×Flag-KDELR1-mCherry, HeLa S3 cells were seeded on a 24 well glass-bottom plate (Cellvis) coated with fibro-nectin (Millipore). After 18 hours transfection with 3xFlag-KDELR1-mCherry and indicated plasmid, cells were incubated with anti-Flag antibody (Sigma) in DMEM with 2% FBS in 4 °C for 1 hour. The cells were washed twice with ice-cold PBS, and then fixed using 4% PFA. After three times washing with PBS, the cells were incubated with secondary antibody for 1 hour. Cells were washed three times and then were imaged with a 63x objective on a Zeiss LSM 880 confocal microscope.

Live cell imaging

For photoactivation experiments, HT1080 WT or ACBD3 stably knockdown cells were seeded on a glass-bottom dish (35 mm diameter, Cellvis) coated with fibronectin (Millipore). After 18 hours co-transfection with KDELR1-PA-GFP and indicated mCherry-Rab, cells were imaged with a 63x objective on a Zeiss LSM 880 confocal microscope in an atmosphere of 5% CO₂ at 37°C. Photoactivating KDELR1-PA-GFP in the Golgi was achieved by using a 405-nm laser. Images were acquired every 5 seconds for 5 min.

Image processing and statistical analysis

Results are displayed as mean ± SD (standard deviation) of results from each experiment or dataset, as indicated in figure legends. All statistical tests were performed using Students T tests or ANOVA (GraphPad, Prism). Significance values are assigned in specific experiments. N (number of individual experiments) is noted in the figure legends.

Supplementary Materials: The following supporting information can be downloaded at the website of this paper posted on Preprints.org.

Author Contributions: Q.Y, X.Y and I.L conceptualized the project and designed the experiments. C.T, Y.D, L.Z, S.J, J.G, X.Y performed the experiments. Q.Y, X.Y and I.L wrote and edited the manuscripts.

Acknowledgments: Financial support of this study was provided by ShanghaiTech University.

Declarations: The authors declare that they have no conflicts of interest with the contents of this article.

Data availability statement: All materials and data supporting this study are available from the corresponding authors (yuexh@shanghaitech.edu; qianyi@shanghaitech.edu; leeintaek@shanghaitech.edu) upon reasonable request.

References

1. Warren, G., and Malhotra, V. (1998) The organisation of the Golgi apparatus. *Curr Opin Cell Biol* **10**, 493-498
2. Kulkarni-Gosavi, P., Makhoul, C., and Gleeson, P. A. (2019) Form and function of the Golgi apparatus: scaffolds, cytoskeleton and signalling. *FEBS Lett* **593**, 2289-2305
3. Munro, S., and Pelham, H. R. (1987) A C-terminal signal prevents secretion of luminal ER proteins. *Cell* **48**, 899-907
4. Pelham, H. R. (1988) Evidence that luminal ER proteins are sorted from secreted proteins in a post-ER compartment. *EMBO J* **7**, 913-918
5. Lewis, M. J., Sweet, D. J., and Pelham, H. R. (1990) The ERD2 gene determines the specificity of the luminal ER protein retention system. *Cell* **61**, 1359-1363
6. Yue, X., Qian, Y., Zhu, L., Gim, B., Bao, M., Jia, J., Jing, S., Wang, Y., Tan, C., Bottanelli, F., Ziltener, P., Choi, S., Hao, P., and Lee, I. (2021) ACBD3 modulates KDEL receptor interaction with PKA for its trafficking via tubulovesicular carrier. *BMC Biol* **19**, 194
7. Cancino, J., Jung, J. E., and Luini, A. (2013) Regulation of Golgi signaling and trafficking by the KDEL receptor. *Histochem Cell Biol* **140**, 395-405
8. Henderson, M. J., Richie, C. T., Airavaara, M., Wang, Y., and Harvey, B. K. (2013) Mesencephalic astrocyte-derived neurotrophic factor (MANF) secretion and cell surface binding are modulated by KDEL receptors. *J Biol Chem* **288**, 4209-4225
9. Becker, B., Shaebani, M. R., Rammo, D., Bubel, T., Santen, L., and Schmitt, M. J. (2016) Cargo binding promotes KDEL receptor clustering at the mammalian cell surface. *Sci Rep* **6**, 28940
10. Bauer, A., Santen, L., Schmitt, M. J., Shaebani, M. R., and Becker, B. (2020) Cell-type-specific differences in KDEL receptor clustering in mammalian cells. *PLoS One* **15**, e0235864
11. Jia, J., Yue, X., Zhu, L., Jing, S., Wang, Y., Gim, B., Qian, Y., and Lee, I. (2021) KDEL receptor is a cell surface receptor that cycles between the plasma membrane and the Golgi via clathrin-mediated transport carriers. *Cell Mol Life Sci* **78**, 1085-1100
12. Lamber, E. P., Siedenburg, A. C., and Barr, F. A. (2019) Rab regulation by GEFs and GAPs during membrane traffic. *Curr Opin Cell Biol* **59**, 34-39
13. Barr, F., and Lambright, D. G. (2010) Rab GEFs and GAPs. *Curr Opin Cell Biol* **22**, 461-470
14. Novick, P. (2016) Regulation of membrane traffic by Rab GEF and GAP cascades. *Small GTPases* **7**, 252-256
15. Progida, C., and Bakke, O. (2016) Bidirectional traffic between the Golgi and the endosomes - machineries and regulation. *J Cell Sci* **129**, 3971-3982
16. De Matteis, M. A., and Luini, A. (2008) Exiting the Golgi complex. *Nat Rev Mol Cell Biol* **9**, 273-284
17. Saimani, U., and Kim, K. (2017) Traffic from the endosome towards trans-Golgi network. *Eur J Cell Biol* **96**, 198-205
18. Johannes, L., and Wunder, C. (2011) Retrograde transport: two (or more) roads diverged in an endosomal tree? *Traffic* **12**, 956-962
19. Cabrera, M., Muniz, M., Hidalgo, J., Vega, L., Martin, M. E., and Velasco, A. (2003) The retrieval function of the KDEL receptor requires PKA phosphorylation of its C-terminus. *Mol Biol Cell* **14**, 4114-4125
20. Cancino, J., Capalbo, A., Di Campli, A., Giannotta, M., Rizzo, R., Jung, J. E., Di Martino, R., Persico, M., Heinklein, P., Sallese, M., and Luini, A. (2014) Control systems of membrane transport at the interface between the endoplasmic reticulum and the Golgi. *Dev Cell* **30**, 280-294
21. Bard, F., Mazelin, L., Pechoux-Longin, C., Malhotra, V., and Jurdic, P. (2003) Src regulates Golgi structure and KDEL receptor-dependent retrograde transport to the endoplasmic reticulum. *J Biol Chem* **278**, 46601-46606
22. Pulvirenti, T., Giannotta, M., Capestrano, M., Capitani, M., Pisanu, A., Polishchuk, R. S., San Pietro, E., Beznoussenko, G. V., Mironov, A. A., Turacchio, G., Hsu, V. W., Sallese, M., and Luini, A. (2008) A traffic-activated Golgi-based signalling circuit coordinates the secretory pathway. *Nat Cell Biol* **10**, 912-922
23. Yang, J. S., Lee, S. Y., Gao, M., Bourgoin, S., Randazzo, P. A., Premont, R. T., and Hsu, V. W. (2002) ARFGAP1 promotes the formation of COPI vesicles, suggesting function as a component of the coat. *J Cell Biol* **159**, 69-78
24. Aoe, T., Cukierman, E., Lee, A., Cassel, D., Peters, P. J., and Hsu, V. W. (1997) The KDEL receptor, ERD2, regulates intracellular traffic by recruiting a GTPase-activating protein for ARF1. *EMBO J* **16**, 7305-7316
25. Majoul, I., Straub, M., Hell, S. W., Duden, R., and Soling, H. D. (2001) KDEL-cargo regulates interactions between proteins involved in COPI vesicle traffic: measurements in living cells using FRET. *Dev Cell* **1**, 139-153
26. Daro, E., van der Sluijs, P., Galli, T., and Mellman, I. (1996) Rab4 and cellubrevin define different early endosome populations on the pathway of transferrin receptor recycling. *Proc Natl Acad Sci U S A* **93**, 9559-9564

27. Sonnichsen, B., De Renzis, S., Nielsen, E., Rietdorf, J., and Zerial, M. (2000) Distinct membrane domains on endosomes in the recycling pathway visualized by multicolor imaging of Rab4, Rab5, and Rab11. *J Cell Biol* **149**, 901-914

28. D'Souza, R. S., Semus, R., Billings, E. A., Meyer, C. B., Conger, K., and Casanova, J. E. (2014) Rab4 orchestrates a small GTPase cascade for recruitment of adaptor proteins to early endosomes. *Curr Biol* **24**, 1187-1198

29. Doray, B., Ghosh, P., Griffith, J., Geuze, H. J., and Kornfeld, S. (2002) Cooperation of GGAs and AP-1 in packaging MPRs at the trans-Golgi network. *Science* **297**, 1700-1703

30. Doray, B., Lee, I., Knisely, J., Bu, G., and Kornfeld, S. (2007) The gamma/sigma1 and alpha/sigma2 hemicomplexes of clathrin adaptors AP-1 and AP-2 harbor the dileucine recognition site. *Mol Biol Cell* **18**, 1887-1896

31. Lee, I., Doray, B., Govero, J., and Kornfeld, S. (2008) Binding of cargo sorting signals to AP-1 enhances its association with ADP ribosylation factor 1-GTP. *J Cell Biol* **180**, 467-472

32. Hirsch, D. S., Stanley, K. T., Chen, L. X., Jacques, K. M., Puertollano, R., and Randazzo, P. A. (2003) Arf regulates interaction of GGA with mannose-6-phosphate receptor. *Traffic* **4**, 26-35

33. Shiba, T., Kawasaki, M., Takatsu, H., Nogi, T., Matsugaki, N., Igarashi, N., Suzuki, M., Kato, R., Nakayama, K., and Wakatsuki, S. (2003) Molecular mechanism of membrane recruitment of GGA by ARF in lysosomal protein transport. *Nat Struct Biol* **10**, 386-393

34. Scott, P. M., Bilodeau, P. S., Zhdankina, O., Winistorfer, S. C., Hauglund, M. J., Allaman, M. M., Kearney, W. R., Robertson, A. D., Boman, A. L., and Piper, R. C. (2004) GGA proteins bind ubiquitin to facilitate sorting at the trans-Golgi network. *Nat Cell Biol* **6**, 252-259

35. Yamamoto, H., Koga, H., Katoh, Y., Takahashi, S., Nakayama, K., and Shin, H. W. (2010) Functional cross-talk between Rab14 and Rab4 through a dual effector, RUFY1/Rabip4. *Mol Biol Cell* **21**, 2746-2755

36. Mohrmann, K., Gerez, L., Oorschot, V., Klumperman, J., and van der Sluijs, P. (2002) Rab4 function in membrane recycling from early endosomes depends on a membrane to cytoplasm cycle. *J Biol Chem* **277**, 32029-32035

37. Yudowski, G. A., Putthenveedu, M. A., Henry, A. G., and von Zastrow, M. (2009) Cargo-mediated regulation of a rapid Rab4-dependent recycling pathway. *Mol Biol Cell* **20**, 2774-2784

38. Roberts, M., Barry, S., Woods, A., van der Sluijs, P., and Norman, J. (2001) PDGF-regulated rab4-dependent recycling of alphavbeta3 integrin from early endosomes is necessary for cell adhesion and spreading. *Curr Biol* **11**, 1392-1402

39. Perez Bay, A. E., Schreiner, R., Benedicto, I., Paz Marzolo, M., Banfelder, J., Weinstein, A. M., and Rodriguez-Boulan, E. J. (2016) The fast-recycling receptor Megalin defines the apical recycling pathway of epithelial cells. *Nat Commun* **7**, 11550

40. Giannotta, M., Ruggiero, C., Grossi, M., Cancino, J., Capitani, M., Pulvirenti, T., Consoli, G. M., Geraci, C., Fanelli, F., Luini, A., and Sallese, M. (2012) The KDEL receptor couples to Galphaq/11 to activate Src kinases and regulate transport through the Golgi. *EMBO J* **31**, 2869-2881

41. McPhail, J. A., Ottosen, E. H., Jenkins, M. L., and Burke, J. E. (2017) The Molecular Basis of Aichi Virus 3A Protein Activation of Phosphatidylinositol 4 Kinase IIIbeta, PI4KB, through ACBD3. *Structure (London, England : 1993)* **25**, 121-131

42. Xiao, X., Lei, X., Zhang, Z., Ma, Y., Qi, J., Wu, C., Xiao, Y., Li, L., He, B., and Wang, J. (2017) Enterovirus 3A facilitates viral replication by promoting PI4KB-ACBD3 interaction. *J Virol*

43. Klima, M., Toth, D. J., Hexnerova, R., Baumlova, A., Chalupska, D., Tykvert, J., Rezabkova, L., Sengupta, N., Man, P., Dubankova, A., Humpolickova, J., Nencka, R., Neverka, V., Balla, T., and Boura, E. (2016) Structural insights and in vitro reconstitution of membrane targeting and activation of human PI4KB by the ACBD3 protein. *Sci Rep* **6**, 23641

44. Ruggiero, C., Grossi, M., Fragassi, G., Di Campli, A., Di Ilio, C., Luini, A., and Sallese, M. (2018) The KDEL receptor signalling cascade targets focal adhesion kinase on focal adhesions and invadopodia. *Oncotarget* **9**, 10228-10246

45. Solis, G. P., Bilousov, O., Koval, A., Luchtenborg, A. M., Lin, C., and Katanaev, V. L. (2017) Golgi-Resident Galphao Promotes Protrusive Membrane Dynamics. *Cell* **170**, 939-955 e924

46. Li, Z., Zhang, L., Zhao, Y., Li, H., Xiao, H., Fu, R., Zhao, C., Wu, H., and Li, Z. (2013) Cell-surface GRP78 facilitates colorectal cancer cell migration and invasion. *Int J Biochem Cell Biol* **45**, 987-994

47. Song, D., Liu, H., Wu, J., Gao, X., Hao, J., and Fan, D. (2021) Insights into the role of ERp57 in cancer. *J Cancer* **12**, 2456-2464

48. Yuan, X. P., Dong, M., Li, X., and Zhou, J. P. (2015) GRP78 promotes the invasion of pancreatic cancer cells by FAK and JNK. *Mol Cell Biochem* **398**, 55-62

49. Orsetti, B., Nugoli, M., Cervera, N., Lasorsa, L., Chuchana, P., Rouge, C., Ursule, L., Nguyen, C., Bibeau, F., Rodriguez, C., and Theillet, C. (2006) Genetic profiling of chromosome 1 in breast cancer: mapping of regions of gains and losses and identification of candidate genes on 1q. *Br J Cancer* **95**, 1439-1447

50. Huang, Y., Yang, L., Pei, Y. Y., Wang, J., Wu, H., Yuan, J., and Wang, L. (2018) Overexpressed ACBD3 has prognostic value in human breast cancer and promotes the self-renewal potential of breast cancer cells by activating the Wnt/beta-catenin signaling pathway. *Experimental cell research* **363**, 39-47

51. Waugh, M. G. (2014) Amplification of Chromosome 1q Genes Encoding the Phosphoinositide Signalling Enzymes PI4KB, AKT3, PIP5K1A and PI3KC2B in Breast Cancer. *J Cancer* **5**, 790-796

52. Frittoli, E., Palamidessi, A., Marighetti, P., Confalonieri, S., Bianchi, F., Malinverno, C., Mazzarol, G., Viale, G., Martin-Padura, I., Garre, M., Parazzoli, D., Mattei, V., Cortellino, S., Bertalot, G., Di Fiore, P. P., and Scita, G. (2014) A RAB5/RAB4 recycling circuitry induces a proteolytic invasive program and promotes tumor dissemination. *J Cell Biol* **206**, 307-328

53. Boulay, P. L., Schlienger, S., Lewis-Saravalli, S., Vitale, N., Ferbeyre, G., and Claing, A. (2011) ARF1 controls proliferation of breast cancer cells by regulating the retinoblastoma protein. *Oncogene* **30**, 3846-3861

54. Morrow, A. A., Alipour, M. A., Bridges, D., Yao, Z., Saltiel, A. R., and Lee, J. M. (2014) The lipid kinase PI4KIIIbeta is highly expressed in breast tumors and activates Akt in cooperation with Rab11a. *Mol Cancer Res* **12**, 1492-1508